STM JOURNALS

Research & Reviews: A Journal of
Drug Design & Discovery

ISSN: 2349-9036
Volume 13, Issue 2, 2026
May–August
DOI (Journal): 10.37591/RRJoDDD

https://journals.stmjournals.com/rrjoddd

Research RRJoDDD

In Silico Identification of Therapeutic Agents for Dengue Virus by Molecular Docking

Peri Shyamalambica[1],*, Adithya Nukala[2]

Abstract

The dengue virus causes serious health issues and a loss of quality of life. Dengue poses a yearly threat to half of the world's population. The drugs that are based on allopathy are expensive and also exhibit toxic effects on tissues and biological activities. It is also generally accepted that most pharmacologically active drugs, including those derived from medicinal plants, are isolated from natural sources. The present study is directed toward identifying an inhibitor of the non-structural protein (dengue virus type 2 genome polyprotein), as no medicines for treating these arboviruses exhibit antiviral activity. To forecast potential high-affinity, selective binders, the biological target's structure was selected. The ProtParam determines the protein's main characteristics. The homology modeling tool MODELER is used to build the non-structural protein's three-dimensional structure using several existing non-structural protein structures as templates. After that, the structure is thoroughly optimized and verified using PROCHECK and VERIFY3D. The receptor's molecular binding active sites were examined using the CASTp server. The non-structural protein's expected structure will serve as a basis for the development of potent inhibitors that may one day be used as natural therapeutics.

Keyword: Dengue virus, non-structural protein 2, homology modeling, ligand, protein ligand interaction profiler

INTRODUCTION

In recent years, the incidence of dengue worldwide has increased. The cases reported by the WHO from 2000 to 2019 are 505, 430 and 5.2 million, respectively. Mild, self-asymptomatic cases are primarily managed. Hence, dengue cases are underreported, and many cases are misguided, just like other febrile illnesses. The highest number of dengue cases was reported in 2023, affecting 80 countries across all WHO regions. These findings, along with the unexpected increase in dengue cases, a historic rise of over 6.5 million cases, and dengue deaths are more than 7300, show that the dengue transmission had begun in early 2023. The WHO estimates that half of the world's population is at risk of contracting dengue each year. The majority of dengue cases occur in metropolitan and semi-urban regions, as well as in tropical and subtropical climates [1-26].

***Author for Correspondence**
Peri Shyamalambica
Email id: shyamalambicaperi1990@gmail.com

[1]Project Scientst, Department of Marine Living Resources, Andhra University, Visakhapatnam, Andhra Pradesh, India
[2]Assistant Professor, Department of CSE, COER University, Roorkee, Uttarakhand, India

Submission Date: January 30, 2026
Acceptance Date: March 17, 2026
Published Date: April 04, 2026

Citation: Peri Shyamalambica, Adithya Nukala. In Silico Identification of Therapeutic Agents for Dengue Virus by Molecular Docking. Research & Reviews: A Journal of Drug Design & Discovery. 2026; 13(2): 1–14p.

The dengue virus, a member of the Flavivirus genus, is a subfamily of the Flavivirdae family. Among the most important human pathogens are Japanese encephalitis virus, a member of the flavivirus group; West Nile Virus (WNV); tick-borne encephalitis virus (TBEV); and Yellow Fever Virus [1]. Flaviviruses are single-stranded, enveloped viruses with a ~11-kb positive-sense RNA genome. The 51 and 31 untranslated regions (UTRs) and single, open reading frames encode the genome [2]. The receptor-mediated endocytosis of the virus involves internalization, acidification, viral fusion, and membrane vesicular trafficking, allowing the release of the genomic RNA into the cytoplasm, which is mRNA [2].

Dengue virus also belongs to the arbovirus group, which is arthropod-borne; the four families that belong to the Togaviridae, Reoviridae, Flaviviridae, and Bunyaviridae share the main Characteristics: the reservoir hosts are transmitted between arthropod vectors to vertebrates in the cycle. Over 700, 000 people die each year from infectious diseases, of which more than 17% are vector-borne [3]. In the large segment of our population, it causes serious health issues and a loss of quality of life, resulting in a significant negative impact on the economy and society [3]. The host immune response, regulation and maturation, proteolysis, assembly, and replication are the intercellular aspects of the viral cycle coordinated by Nonstructural Proteins (NS), as no medicines for treating these arboviruses show antiviral activity. The most commonly prescribed drugs, like acetaminophen and non-steroidal anti-inflammatories, can lead to internal bleeding and hemorrhages. Therefore, it is necessary to develop effective therapeutic activities by combining low cost and high specificity to improve the patient's quality of life [3].

The plant or natural product is therapeutic for many diseases and is used for disease management. It is still under active research due to its lower affordability and potential side effects. Plant products are essential for enhancing antioxidant activity, modulating genetic pathways, and inhibiting bacterial growth to prevent and treat diseases. The drugs that are based on allopathy are expensive and also exhibit toxic effects on tissues and biological activities [28-50]. It is also generally accepted that most pharmacologically active drugs, including those derived from medicinal plants, are isolated from natural sources [4].

In modern times, the traditional medicinal system is impressive, as it has been a source of medicinal agents for thousands of years, with natural sources isolated only from where they are obtained [5]. Especially in Indian Ayurvedic, Unani, and Homoeopathic medicine, the seeds, leaves, bark, roots, fruits, and oil of Azardirachta indica are used to treat a variety of diseases [6]. Both developed and developing nations investigated the biological activity and chemical components of Azardirachta indica. [5].

The neem bark extract significantly blocks HSV-1 entry into cells at the tested concentration. It has a direct anti-HSV-1 property; the extract blocks NBE activity when the virus is preincubated in the extract, but not in the presence of target cells [6]. Neem leaf extract has virucidal activity against Coxsackievirus B-4, resulting in virus inactivation [4].

Bioinformatics techniques are used across a broad spectrum to evaluate intrinsic disorders in the complete proteomes of four human dengue virus (DENV) genotypes, to analyze the peculiarities of disorder distribution within individuals' DENV proteins, and to establish potential roles for structural disorder in their functions.

The complete proteomes of the four human dengue virus (DENV) genotypes are evaluated using a wide range of bioinformatics techniques. This enables analysis of the unique distribution of structural disorders within each person's DENV proteins and the identification of possible roles for these disorders in their functions. Along with the dengue fever virus, hepatitis C virus, West Nile virus, and yellow fever virus, the family Flaviviridae belongs to the genus Flavivirus.

Most of the over 80 viruses that make up the flavivirus genus are arthropod-borne human pathogens that cause a range of illnesses, including dengue fever and its related conditions, dengue hemorrhagic fever and dengue shock syndrome, Yellow fever, and Japanese encephalitis [7]. The dengue virus has four antigenically related serotypes (DEBV-1, 2, 3, 4). All these serotypes are known to cause a full-spectrum disease [8].

Lifelong immunity is conferred by infection with one of these serotypes, but only to the serotypes [9]. Therefore, in a dengue-endemic area, individuals are at risk of secondary infection with other DENV serotypes. Dengue virus is an arthropod-borne virus (arbovirus) primarily transmitted between *Aedes aegypti* and humans, which breeds in domestic and peridomestic water containers.

In Southeast Asia and West Africa, a sylvatic cycle, in which jungle primates and mosquito vectors spread the virus, has been observed; however, the extent to which this cycle contributes to human infection is currently unknown [10]. *Aedes* mosquitoes, which develop in tree holes and spread the virus from monkey to monkey, from monkey to human, and between humans, are thought to be involved in the enzootic maintenance cycle of this virus.

It is also documented in West Africa, Sri Lanka, and Malaysia that the dengue virus has zoonotic cycles, with transmission involving forest *Aedes* species and monkeys. *Aedes niveus* is a vector in Malaysia; *Aedes furcifer* is a species implicated in West Africa; *Aedes aegypti*, *Aedes taylori*, *Aedes opok*, and *Aedes luteocephalus*. The most important vector is *Aedes aegypti*; other *Aedes* species also play an essential role in disease transmission [7]. Another member of the flavivirus genus, *Aedes* flavivirus, also shows vertical transmission from mosquito to mosquito. Around 2.5 billion individuals in tropical regions are thought to be at risk of contracting dengue, and each year there are 100 million cases of dengue fever and 250, 000 cases of dengue hemorrhagic fever reported globally [7].

Hemorrhagic fever, dengue shock syndrome, and mild subclinical symptoms are among the most common clinical manifestations of dengue virus infection. Nonspecific febrile illness, classic dengue fever, dengue hemorrhagic fever (grades I and II), and dengue shock syndrome (grades III and IV) are the severity-based classifications for the disease [11].

The most common sign of classic dengue fever is a rapid onset of fever accompanied by several symptoms, including leukopenia, headache, retro-orbital discomfort, myalgia, arthralgia, and hemorrhagic features [12]. In this molecular docking study, 15 natural or plant products were tested against the dengue virus therapeutic target protein, the envelope protein. The drug design process is in silico, which involves the identification and testing of therapeutic targets and the screening of small molecules against them [13]. After that, docking the smaller molecules from the library initiates virtual screening. The chemicals that pass these detailed profiling investigations are referred to as leads. These selected findings are tested for specificity by docking at binding sites of established medication targets [14].

MATERIALS AND METHODS

Sequence Retrieval

The NCBI's protein database was used to obtain the amino acid sequences of the dengue virus type 2 genome polyprotein (Accession P12823.1). The 3, 388-amino-acid protein is used in this study for additional research (Figure 1).

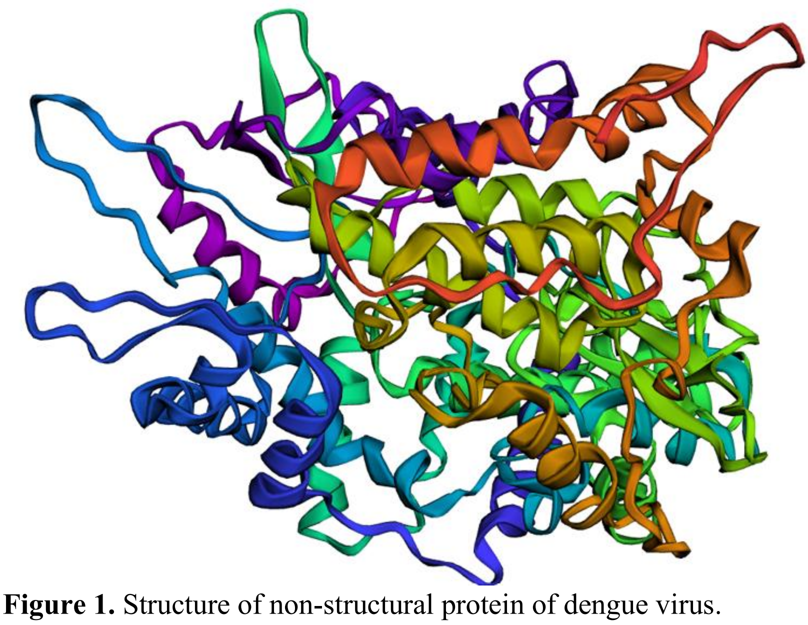

Figure 1. Structure of non-structural protein of dengue virus.

Primary Structure Prediction

The protein's physicochemical properties were calculated using ExPASy's ProtParam program [5]. The theoretical isoelectric point (pI), molecular weight, total number of positive and negative residues, extinction coefficient [15], instability index [16], aliphatic index [17], and grand average hydropathicity (GRAVY) of the protein were all calculated using the default parameters (Table 1).

Table 1. Different physicochemical properties of nonstructural protein 2 of dengue virus.

Parameters	Value
Molecular weight	70511.38.
Extinction coefficient Abs 0.1%(=1g/1)1.033, assuming all pairs of Cys residues form cystines	68435.
Extinction coefficient Abs 0.1%(=1g/1)1.013, assuming all Cys residues are reduced	66810.
Theoretical pI	6.25.
Total number of negatively charged residues (Asp + Glu):	74.
Total number of positively charged residues (Arg + Lys):	70.
Instability index	36.06.
Grand average of hydropathicity (GRAVY)	-0.062.
Aliphatic index	88.93.

TEMPLATE SELECTION

To identify a good template for the protein, BLAST is used. BLAST results indicate the degree of similarity between a protein with unknown structures and those found in the Protein Data Bank [18]. With 100% query coverage, 1oke_A/B was determined to be the best homolog for nonstructural protein 2 using BLAST. PDB was used to obtain the structural summary for the homology. Figure 2 displays the BLAST's outcome.

Figure 2. Genome polyprotein 2 BLAST.

HOMOLOGY MODELING

A comparative modeling application, MODELLER 9.20 [19], was used to generate the model. It creates a modified three-dimensional homology model of a protein sequence using a selected template and a provided sequence alignment. Given the close relationship between the query and template

Research & Reviews: A Journal of Drug Design & Discovery
Volume 13, Issue 2
ISSN: 2349-9036

molecules, homology modeling can yield high-quality models. Protein structures are more conserved than their sequences when the identity is greater than 20%; however, model quality may suffer if the target and template sequence identity is less than 20% [20]. Based on the lowest discrete optimized protein energy (DOPE) score and highest GA341 score, the MODELLER produced five structures using 1oke_A as the template, and the best one was selected [21].

Ligand's Preparation

As ligand molecules, a few natural medicinal compounds and their analogs were taken from the PubChem compound database maintained by the National center for Biotechnology Information (NCBI). Open Babel was used to translate these molecules from the SDF (structure data file) format to Protein Data Bank (PDB) coordinates. After submitting the chosen ligand molecules to the Molinspiration server, Lipinski's Rule of Five was used to determine how likely they were to exhibit drug-like characteristics. For additional analysis, only the molecules that passed this filter were used. The ideal medicine molecule should weigh less than 500 moles, have fewer than five hydrogen bonds overall, have a miLogP value of less than five, and have a sum of N and O of no more than ten [15] (Table 2).

Table 2. Molecular properties of ligand molecules identified by the molinspiration server.

Ligand	miLogP	TPSA	Natoms	MW	nON	NOHNH	n violations	Nrotb	Volume
1	2.85	112.28	36	498.57	8	1	0	6	452.45
2	3.66	86.11	34	466.57	6	0	0	3	430.17
3	1.05	86.99	25	350.45	5	3	0	3	338.33
4	1.38	41.12	16	224.35	3	2	0	4	236.41
5	5.40	110.52	43	596.72	9	0	2	9	551.94
6	0.86	23.55	16	224.35	3	0	0	4	236.69
7	1.72	66.76	24	334.46	4	2	0	4	330.29
8	4.34	95.35	35	485.57	7	0	0	3	439.15
9	1.17	125.69	34	480.60	8	4	0	7	454.37
10	2.04	134.27	34	470.52	8	3	0	4	417.39
11	1.83	100.13	32	442.55	6	3	0	1	408.10
12	3.55	118.36	39	540.61	9	0	1	8	488.96
13	1.94	92.06	34	466.53	7	0	0	4	417.03
14	2.15	175.51	45	632.75	11	5	2	6	574.50
15	4.15	96.36	34	470.61	6	2	0	2	441.81

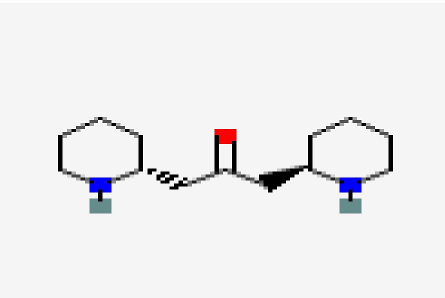

Anaferine

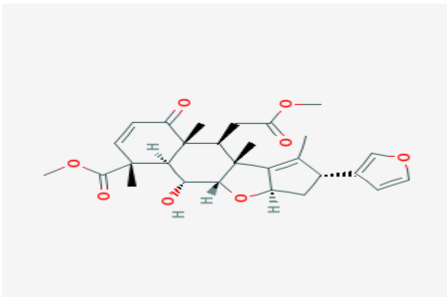

6 Deacetylnimbine

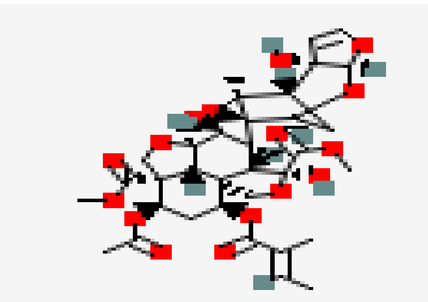

Azadirachtin

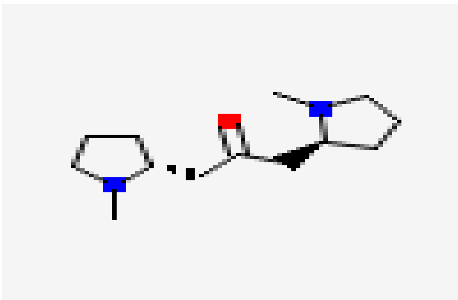

Cuscohygrine

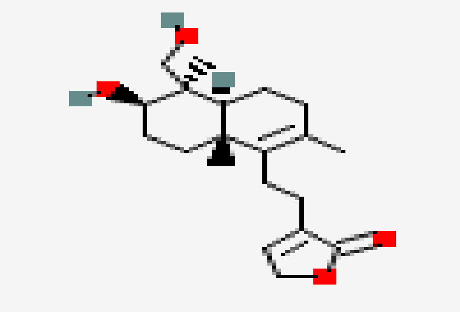
Deoxyandrographolide

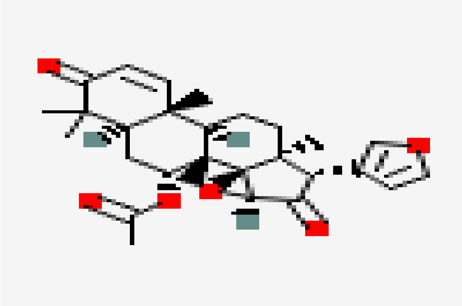
Epoxyazadiradione

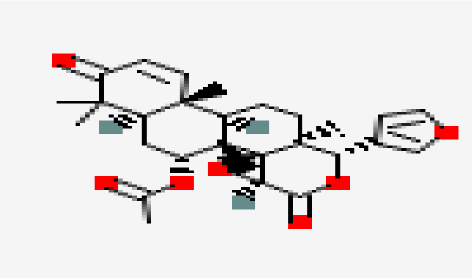
Gedunin

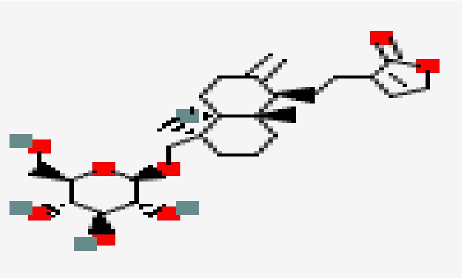
Neoandrographol

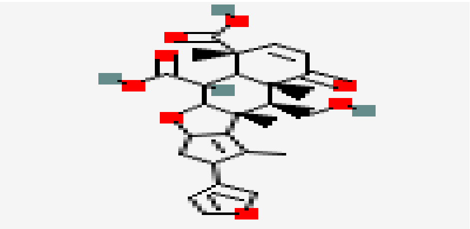
Nimbic Acid

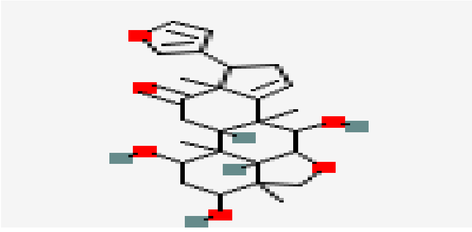
Nimbidinin

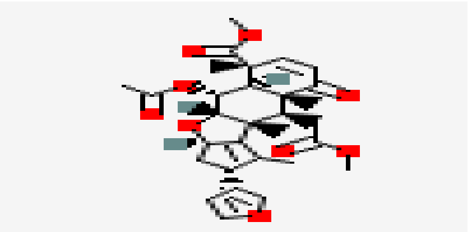
Nimbin

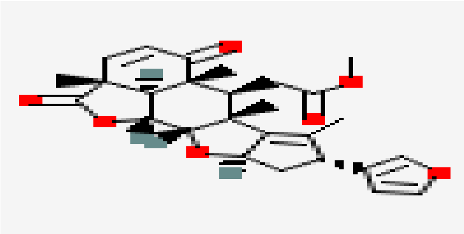
Nimbolide

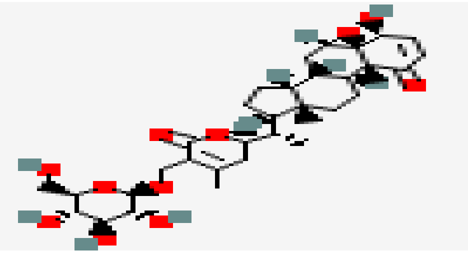
Sitoindosides IX

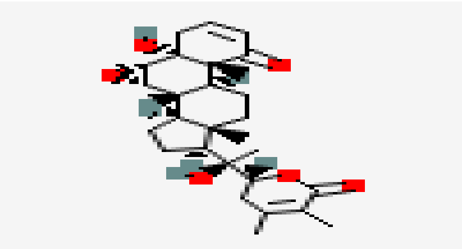
Withanolide A

Verification and Validation of the Structure

The accuracy and stereochemical features of the predicted model were assessed using PROCHECK [22] and the Ramachandran plot analysis [8], which were performed through the SAVESv6.0 server (servicesn.mbiuda.edu/SAVES/). The number of residues in the core, allowed, generously allowed, and disallowed regions, as well as the total G-factor, were used to choose the most effective model (Figures 3 and 4] (Table 3).

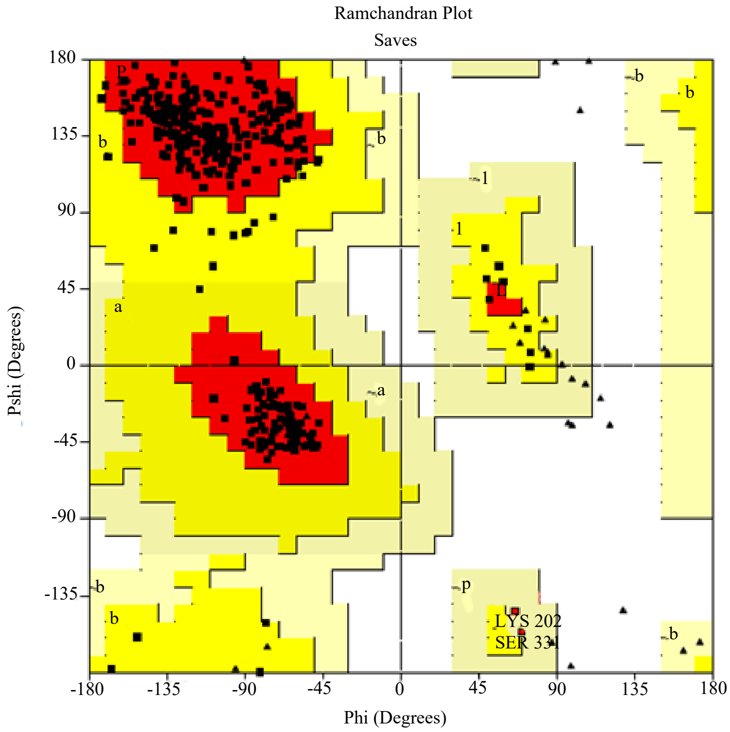

Figure 3. Ramachandran plot analysis of selected model.

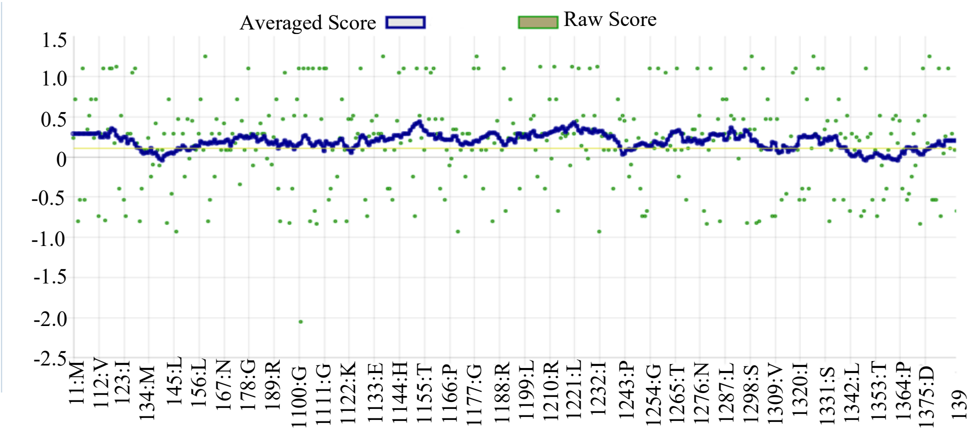

Figure 4. Verify 3D of non-structural protein 2 of dengue virus.

Table 3. Ramachandran plot of Non-structural protein 2 from dengue virus.

Ramachandran plot statistics	**Non-structural protein 2**	
	Residue	**%**
Residues in the most favored regions[A,B,L]	308	91.7
Residues in the additional allowed regions [a,b,l,p]	26	7.7
Residues in the generously allowed regions [a,b,l,p]	2	0.6
Residues in the disallowed regions [xx]	0	0.0
Number of non-glycine and non-proline residues	336	100.0
Number of end residues (excl.Gly and PRO)	2	
Number of glycine residues	37	
Number of proline residues	19	
Total number of residues	394	

Active Site Analysis

The Computed Atlas of Surface Topography of Proteins (CASTp) server was used to determine potential binding sites after the three-dimensional structure of non-structural protein 2 was modelled. This was done to evaluate the structural alignment between the model and the template [12]. Binding sites, surface structural pockets, active sites, and the area, shape, and volume of each pocket and internal cavity in proteins were all identified and described using CASTp3.0. Additionally, it might be used to determine each pocket's area, accessible molecular surface, number, and mouth-opening [29]. An essential source of information about the docking simulation is active-site analysis.

Docking Simulation Study

An in silico docking simulation study was conducted to recognize the inhibiting potential against non-structural protein 2. AutoDock Vina and AutoDock 1.5.6 were used for the docking study. Polar hydrogen was added to non-structural protein 2 before the docking simulation investigation. All compounds were screened using AutoDock Vina version 1.5.6 to search for chemicals with high binding affinities for non-structural protein 2. The size of the grid box was set as center_x = 109.682, center_y = 115.301, center_z = 125.648, size_x = 78, size_y = 78, size_z = 126. The exhaustiveness level was set to 8. The compound with the highest binding affinities was then analyzed and considered a possible template for further optimization. Then, AutoDock version 1.5.6 was performed, and the search results were analyzed using the Lamarckian genetic algorithm. A ligand with the lowest binding energy is chosen when ligands are compared according to binding energy [2] (Table 4).

Table 4. Identifying binding affinity between protein and ligand by autodock.

Ligand	**Binding affinity**	**Distance from best mode**	
		Msd Lb	**Msd Ub**
6 desacetyl nimbinene 1	-11.4	0.000	0.000.
6 desacetyl nimbinene 2	-11.3	1.431	6.146.
Azadirachtin 1	-11.6	0.000	0.000.
Azadirachtin 2	-11.2	2.147	4.386.
Anaferine 1	-6.8	0.000	0.000.
Anaferine 2	-6.8	0.017	4.791.
Andrographolide 1	-9.4	0.000	0.000.
Andrographolide 2	-8.3	14.895	17.868.
Cuscohygrine 1	-7.1	0.000	0.000.
Cuscohygrine 2	-7.0	2.116	4.386.
Deoxyandrographolode 1	-9.9	0.000	0.000.
Deoxyandrographolode 2	-9.9	1.650	5.578.
Epoxyazadiradione 1	-14.5	0.000	0.000.
Epoxyazadiradione 2	-13.9	1.827	3.353.
Gedunin 1	-13.6	0.000	0.000.
Gedunin 2	-12.8	2.084	2.908.
Neoandrapholide 1	-9.7	0.000	0.000.
Neoandrapholide 2	-9.7	13.529	17.922.
Nimbic acid 1	-12.3	0.000	0.000.
Nimbic acid 2	-12.1	1.332	2.853
Nimbidinin 1	-11.7	0.000	0.000..
Nimbidinin 2	-11.4	1.579	5.505.
Nimbin 1	-8.6	0.000	0.000.
Nimbin 2	-8.3	24.390	28.096.
Nimbolide 1	-12.9	0.000	0.000.
Nimbolide 2	-12.9	1.147	2.588.
Sitoindosides IX 1	-12.4	0.000	0.000.
Sitoindosides IX 2	-12.2	1.249	1.943.
Withanolides A 1	-8.2	0.000	0.000.
Withanolides A 2	-8.2	14.076	15.600.

RESULTS AND DISCUSSION

The two ligands, namely epoxyazadiradione (8.12 (BE) and 1.11 µM (IC)) and Anaferine (-4.01 (BE) and 1.15 mM (IC)), were highly significant among the 15 ligands, with good binding affinity and inhibition constants. A key component of the structure-based drug design process is docking small-molecule compounds into the binding site of a receptor and calculating the complex's binding affinity. A precise, quick docking procedure and the ability to visualize binding geometries and interactions are essential for a comprehensive understanding of the structural principles that dictate the strength of a protein/ligand complex. To illustrate how docking and visualization can support structure–based drug design efforts, an interface between the molecular docking suites AutoDock 1.5.6 and Vina 1.5.6 and the well-known molecular graphics program PyMOL 1.3 was created for this study.

In this study, we provide a PyMOL 1.3 plugin that facilitates binding site analysis, virtual screening, and molecular docking. The plugin extensively leverages a set of Python scripts to set up docking runs and acts as an interface between PyMoL 1.3 and two well-known docking programs. Autodock 1.5.6 and Autodock Vina 1.5.6. Given the importance of visualization in structure-based drug design, a number of tools have been developed to complement the AutoDock 1.5.6 suite.

The plugin uses scripts from the Autodock 1.5.6 tools package to prepare these files. To identify and describe binding sites, Castp looks for pockets and voids in protein structures. One can either specify a directory containing a library of ligands to be docked or prepare ligands one at a time in PyMoL 1.3 [19] for later docking runs. Autodock docks using interaction maps. These maps are computed using the autogrid program before the docking run [16].

The interaction energy between each type of ligand atom and the receptor is computed for the whole binding site, which is divided into discrete areas using a grid. Both the ranking list of docked ligands and their corresponding binding postures can be exported, and docking poses are ranked by docking score. For example, it is possible to export the prioritized list of docking results in CSV format and import it directly into an application such as Excel.

For the drugs selected from AutoDock, a profiler is used to provide thorough identification and visualization of protein–ligand interactions. Similar to Galaxysite [17] or proBis [25], PLIP is a supplementary web tool that can be used to assess docking data (Figures 5 and 6). A web tool called PLIP enables the identification and visualization of patterns of protein–ligand interactions from three-dimensional structures. The binding relationship between the therapeutic compounds that docked with powerful agents and the targeted protein was examined using the Autodock tools (ADT, version 1.5.6) and PLIP [11]. The protein–ligand interaction is depicted in Figures 7 and 8 (Table 5).

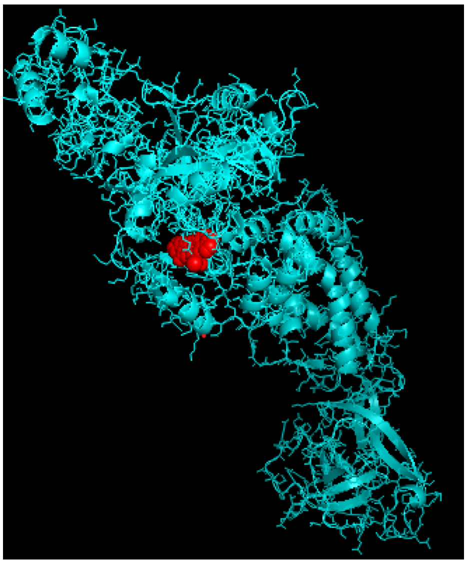

Figure 5. Molecular docking of epoxyazadiradione.

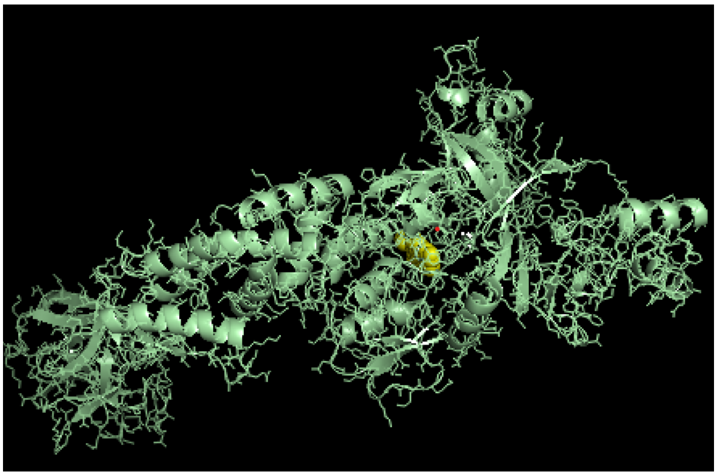

Figure 6. Molecular docking of anaferine.

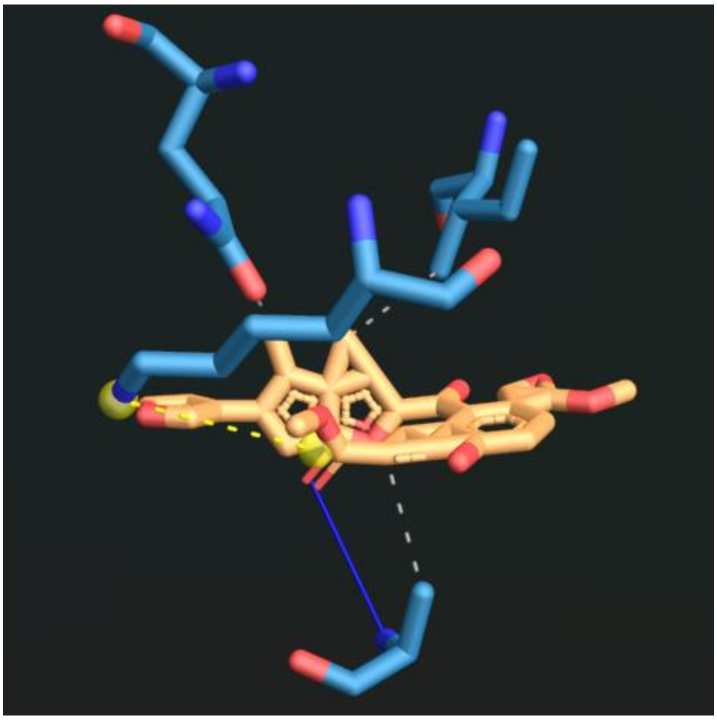

Figure 7. Protein-ligand interaction profiler of epoxyazadiradione.

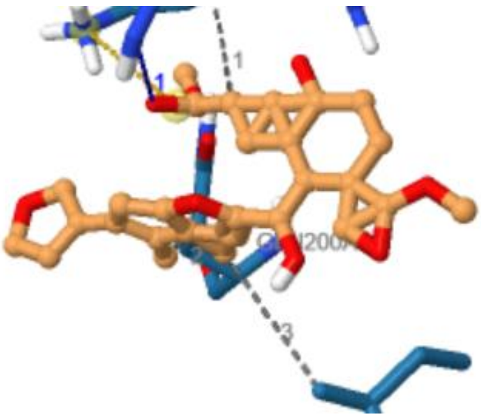

Figure 8. Protein-ligand interaction profiler of anaferine.

Table 5. Molecular simulation by autodock.

Ligand	Binding energy	Ligand_efficiency	Inhib_constant	Inhib_constant_units	Intermol_energy	Vdw_hb_des_energy	Electrostatic_energy	Total_internal	Torsional_energy	Unbound energy	File name	Cl RMS	Ref RMS	Rseed 1	Rseed 2
6 desacetylnimbinene	-7.6	-0.21	2.71	µM	-9.68	-9.65	-0.04	83.81	2.09	83.81	Dock.dlg	0	90.81	none	none
Anaferine	-4.01	-0.25	1.15	mM	-5.2	-3.85	-1.35	18.69	1.19	18.69	Dock.dlg	0	82.66	none	none
Azadirachtin	-8.2	-0.16	979.32	nM	-11.18	-11.07	-0.11	78.02	2.98	78.02	Dock.dlg	0	76.86	none	None
Gedunin	-8.45	-0.24	898.62	nM	-9.34	-9.29	-0.05	16.46	0.89	16.46	Dock.dlg	0	106.04	none	none
Cuscohygrine	-4.82	-0.3	290.77	µM	-5.42	-4.5	-0.92	10.06	0.6	10.06	Dock.dlg	0	93.48	none	none
Deoxyandrographolode	-7.7	-0.32	2.27	µM	-9.14	-9.17	-0.02	82.51	1.49	82.51	Dock.dlg	0	93.07	none	none
Epoxyazadiradione	-8.12	-0.24	1.11	µM	-9.02	-8.91	-0.1	120.91	0.89	120.91	Dock.dlg	0	105.91	none	none
Neoandrapholide	-8.31	-0.24	811.55	nM	-10.99	-10.8	-0.2	12.74	2.68	12.74	Dock.dlg	0	93.09	none	none
Nimbic acid	-10.51	-0.31	19.84	nM	-12.0	-11.99	-0.01	208.8	1.49	208.8	Dock.dlg	0	91.37	none	none
Nimbidinin	-10.9	-0.34	10.22	nM	-12.39	-12.39	0.0	13.18	1.49	13.18	Dock.dlg	0	91.11	none	none
Nimbin	-8.2	-0.21	978.85	nM	-10.29	-10.36	0.08	109.52	2.09	109.52	Dock.dlg	0	89.89	none	none
Nimbolide	-11.02	-0.32	8.3	nM	-11.62	-11.6	-0.02	9.97	0.6	9.97	Dock.dlg	0	92.53	none	none
Sitoindosides IX	-8.29	-0.18	831.8	nM	-11.58	-11.53	-0.05	44.76	3.28	44.76	Dock.dlg	0	84.37	none	none
Withanolides A	-10.69	-0.31	14.5	nM	-11.59	-11.58	0.0	55.19	0.89	55.19	Dock.dlg	94.552	n/a	none	none
Andrographolide	-8.4	-0.34	701.47	nM	-9.59	-9.55	-0.03	10.08	1.19	10.08	Dock.dlg	0	91.75	none	none

CONCLUSION

The popular molecular graphics program PyMOL 1.3 was given a new plugin in this study, which enabled docking studies using AutoDock 1.5.6 or AutoDock Vina 1.5.6. The plugin includes capabilities for planning, carrying out, and evaluating virtual screening positions, in addition to all the features needed for the docking run’s entire workflow. Because structure-based drug design relies heavily on visual support, the plugin is anticipated to improve these efforts by integrating PyMoL 1.3 with two popular docking applications. Fifteen compounds were identified across the articles that inhibited Dengue Virus in the in vitro drug susceptibility assay. Globally, the Dengvaxia vaccine (dengue virus) is the only vaccine currently approved by the U.S., and it is also recommended for a specific population. Since there is no particular drug for the dengue virus, this study aimed to examine drugs that may inhibit the dengue virus non-structural protein 2, which binds to the human prohibitin receptor. The established ligand-based pharmacophore model was used to identify standard features of non-structural protein 2 inhibitors in the PubChem database, and the virtual screening method was used to screen the compound library. After that, molecular docking was used to examine the detailed binding modes of the selected ligands with the active site of non-structural protein 2. The computational approaches showed the advantage of saving time and resources. It is feasible to block the interaction of non-structural protein 2 with the selected 15 compounds using virtual screening based on pharmacophore and molecular docking. Several structurally diverse active compounds were identified in non-structural protein 2 inhibitors of dengue virus. This revealed that the sequential use of available tools, such as AutoDock/Vina, yields better results for blocking the interaction of non-structural protein 2. The docking results were visualized using the software Protein-Ligand Interaction Profiler and Protein Plus. In the following study, two chemical compounds, epoxyazadiradione and Anafarine, were predicted. These compounds, identified by the pharmacophore model, virtual screening, and molecular docking, require further verification through related biological experiments. Such further studies may help identify effective inhibitors of the virus's non-structural protein 2, which does not interact with the human Prohibitin receptor.

REFERENCES

1. Zong A, Cao H, Wang F. Anticancer polysaccharides from natural resources: A review of recent research. Carbohydr Polym. 2012;90(4):1395–1410.
2. Alzohairy MA. Therapeutics role of Azadirachta indica (Neem) and their active constituents in diseases prevention and treatment. Evid Based Complement Alternat Med. 2016;2016:7382506.
3. Angelini MM, Akhlaghpour M, Neuman BW, Buchmeier MJ. Severe acute respiratory syndrome coronavirus nonstructural proteins 3, 4, and 6 induce double-membrane vesicles. mBio. 2013;4(4):e00524–13.
4. Ayyub M, Khazindar AM, Lubbad EH, Barlas S, Alfi AY, Al-Ukayli S. Characteristics of dengue fever in a large public hospital, Jeddah, Saudi Arabia. J Ayub Med Coll Abbottabad. 2006;18:9–13.
5. Azami NAM, Salleh SA, Neoh HM, Zakaria SZS, Jamal R. Dengue epidemic in Malaysia: Not a predominantly urban disease anymore. BMC Res Notes. 2011;4:216.
6. Buendia-Atencio C, Pieffet GP, Montoya-Vargas S, Martinez Bernal JA, Rangel HR, Muñoz AL, et al. Inverse molecular docking study of NS3-helicase and NS5-RNA polymerase of Zika virus as possible therapeutic targets of ligands derived from Marcetia taxifolia and its implications to Dengue virus. ACS Omega. 2021;6(9):6134–6143.
7. Chothia C, Lesk AM. The relation between the divergence of sequence and structure in proteins. EMBO J. 1986;5(4):823–826.
8. Colovos C, Yeates TO. Verification of protein structures: Patterns of nonbonded atomic interactions. Protein Sci. 1993;2:1511–1519.
9. Cornillez-Ty CT, Liao L, Yates JR 3rd, Kuhn P, Buchmeier MJ. Severe acute respiratory syndrome coronavirus nonstructural protein 2 interacts with a host protein complex involved in mitochondrial biogenesis and intracellular signaling. J Virol. 2009;83(19):10314–10318.
10. Dai J, Punchihewa C, Mistry P, Ooi AT, Yang D. Novel DNA bis-intercalation by MLN944, a potent clinical bisphenazine anticancer drug. J Biol Chem. 2004;279:46096–46103.
11. DeLano WL. PyMOL: An open-molecular graphic tool. CCP4 Newsl Protein Crystallogr. 2002;40:82–92.
12. Dundas J, Ouyang Z, Tseng J, Binkowski A, Turpaz Y, Liang J. CASTp: Computed atlas of surface topography of proteins. Nucleic Acids Res. 2006;34:W116–W118.
13. Ekenna C, Fatumo S, Adebiyi E. In-silico evaluation of malaria drug targets. Int J Eng Technol. 2010;2(2):132–135.
14. Eid A, Jaradat N, Elmarzugi N. A review of chemical constituents and traditional usage of Neem plant (Azadirachta indica). Palest Med Pharm J. 2017;2(2):75–81.
15. Eswar N, Marti-Renom MA, Webb B, Madhusudhan MS, Eramian D, Shen M, et al. Comparative protein structure modeling with MODELLER. Curr Protoc Bioinformatics. 2006;15:5.6.1–5.6.30.
16. Franco L, Palacios G, Martinez JA, Vázquez A, Savji N, De Ory F, et al. First report of sylvatic DENV-2-associated dengue hemorrhagic fever in West Africa. PLoS Negl Trop Dis. 2011;5:e1251.
17. Ferreira LG, Santos RN, Oliva G, Andricopulo AD. Molecular docking and structure-based drug design strategies. Molecules. 2015;20:13384–13421.

18. Gebhard LG, Filomatori CV, Gamarnik AV. Functional RNA elements in the dengue virus genome. Viruses. 2011;3(9):1739–1756.
19. Gill SC, von Hippel PH. Calculation of protein extinction coefficients from amino acid sequence data. Anal Biochem. 1989;182(2):319–326.
20. Guruprasad K, Reddy BV, Pandit MW. Correlation between stability of a protein and its dipeptide composition. Protein Eng. 1990;4(2):155–161.
21. Hagar M, Ahmed HA, Aljohani G, Alhaddad OA. Investigation of some antiviral N-heterocycles as COVID-19 drug. Int J Mol Sci. 2020;21(11):3922.
22. Heo L, Shin WH, Lee MS, Seok C. GalaxySite: Ligand-binding-site prediction by using molecular docking. Nucleic Acids Res. 2014;42:W210–W214.
23. AutoDock. How to prepare a grid parameter file for AutoGrid4 [Internet]. Available from: http://autodock.scripps.edu/faqs-help/how-to/how-to-prepare-a-grid-parameter-files-for-autogrid4
24. Ikai A. Thermostability and aliphatic index of globular proteins. J Biochem. 1980;88(6):1895–1898.
25. Konc J, Češnik T, Konc JT, Penca M, Janežič D. ProBiS-database: precalculated binding site similarities. J Chem Inf Model. 2012;52:604–612.
26. Kumar S, Chethan H. An insight to drug designing by in silico approach in biomedical research. J Public Health Med Res. 2013;1(2):63–66.
27. Badam L, Joshi SP, Bedekar SS. In vitro antiviral activity of neem (Azadirachta indica) leaf extract against group B coxsackieviruses. J Commun Dis. 1999;31(2):79–90.
28. Lindenbach BD, Rice CM. Flaviviridae: The viruses and their replication. In: Fields Virology. Philadelphia: Lippincott-Raven; 2007. p. 1101–1152.
29. Louis HM, Hans CA, Xin-zhuan S, Thomas EW. Malaria biology and disease pathogenesis. Nat Med. 2013;19:156–167.
30. Laskowski RA, Rullmannn JA, MacArthur MW, Kaptein R, Thornton JM. AQUA and PROCHECK-NMR. J Biomol NMR. 1996;8:477–486.
31. Narayanaswamy R, Lam KWLK, Ismail IS. Molecular docking analysis of natural compounds as HNE inhibitors. J Chem Pharm Res. 2013;5(10):337–341.
32. Yang P, Wang X. COVID-19: a new challenge for human beings. Cell Mol Immunol. 2020;17:555–557.
33. Maharana S, Wang J, Papadopoulos DK, Richter D, Pozniakovsky A, Poser I, et al. RNA buffers the phase separation behavior of prion-like RNA binding proteins. Science. 2018;360:918–921.
34. Meng F, Badierah RA, Almehdar HA, Redwan EM, Kurgan L, Uversky VN. Unstructural biology of dengue virus proteins. FEBS J. 2015;282(17):3368–3394.
35. Mier-y-Teran-Romero L, Schwartz IB, Cummings DAT. Breaking the symmetry: Immune enhancement increases persistence of dengue viruses. J Theor Biol. 2013;332:203–210.
36. Muratov EN, Amaro R, Andrade CH, Brown N, Ekins S, Fourches D, et al. Computational approaches for COVID-19 drug discovery. Chem Soc Rev. 2021;50(16):9121–9151.
37. Ramachandran GN, Ramakrishnan C, Sasisekharan V. Stereochemistry of polypeptide chain configurations. J Mol Biol. 1963;7:95–99.
38. Ramesh KD, Sanjuktha M, Singaravel S, Ramakrishnan JJ, Rajan KS, Satheesh M, et al. Molecular modelling and docking studies on shrimp vitellogenin receptor. Int J Res Drug Deliv. 2012;2(1):11–14.
39. Rodenhuis-Zybert IA, Wilschut J, Smit JM. Dengue virus life cycle. Cell Mol Life Sci. 2010;67:2773–2786.
40. Sali A, Blundell TA. Comparative protein modelling. J Mol Biol. 1993;234:779–815.
41. Salentin S, Schreiber S, Haupt VJ, Adasme MF, Schroeder M. PLIP: Protein–ligand interaction profiler. Nucleic Acids Res. 2015;43:W443–W447.
42. Sreekanth GP, Chuncharunee A, Sirimontaporn A, Panaampon J, Srisawat C, Morchang A, et al. Role of ERK1/2 signaling in dengue virus-induced liver injury. Virus Res. 2014;188:15–26.
43. Efferth T, Koch E. Complex interactions between phytochemicals. Curr Drug Targets. 2011;12(1):122–132.
44. Tiwari R, Verma AK, Chakraborty S, Dhama K, Singh SV. Neem (Azadirachta indica) and its potential. J Biol Sci. 2014;14(2):110–123.

45. Tseng CH, Lin CK, Chen YL, Hsu CY, Wu HN, Tseng CK, et al. Synthesis and anti-dengue evaluations of quinoline derivatives. Eur J Med Chem. 2014;79:66–76.
46. Tiwari V, Darmani NA, Yue BYJT, Shukla D. In vitro antiviral activity of neem bark extract against HSV-1. Phytother Res. 2010;24(8):1132–1140.
47. Wadood A, Ahmed N, Shah L, Ahmed A, Hassan H, Shams S. In-silico drug design. OA Drug Des Deliv. 2013;1(1):3.
48. Weerakoon KG, Kularatne SA, Edussuriya DH, Kodikara SK, Gunatilake LP, Pinto VG, et al. Histopathological diagnosis of myocarditis in dengue outbreak. BMC Res Notes. 2011;4:268.
49. World Health Organization. World health statistics 2007. Geneva: WHO; 2007.
50. Zhou P, Yang XL, Wang XG, Hu B, Zhang L, Zhang W, et al. A pneumonia outbreak associated with a new coronavirus of probable bat origin.

